The Cryosphere Discuss., 6, 3539–3573, 2012
www.the-cryosphere-discuss.net/6/3539/2012/
doi:10.5194/tcd-6-3539-2012

The Cryosphere Discussions

How does internal variability influence the ability of CMIP5 models to reproduce the recent trend in Southern Ocean sea ice extent?

V. Zunz, H. Goosse, and F. Massonnet

Georges Lemaître Centre for Earth and Climate Research, Earth and Life Institute, Université catholique de Louvain, Louvain-la-Neuve, Belgium

Received: 24 July 2012 – Accepted: 20 August 2012 – Published: 3 September 2012

Correspondence to: V. Zunz (violette.zunz@uclouvain.be)

Published by Copernicus Publications on behalf of the European Geosciences Union.

Abstract

Observations over the last 30 yr have shown that the sea ice extent in the Southern Ocean has slightly increased since 1979. Mechanisms responsible for this positive trend have not been well established yet and climate models are generally unable to simulate correctly this expansion. In this study, we focus on two related hypotheses that could explain the misrepresentation of the positive trend in sea ice extent by climate models: an unrealistic internal variability and an inadequate initialization of the system. For that purpose, we analyze the evolution of sea ice around the Antarctic simulated by 24 different general circulation models involved in the 5th Coupled Model Intercomparison Project (CMIP5). On the one hand, historical simulations, driven by external forcing and initialized without observations, are examined. They provide information about the mean state, the variability and the trend in sea ice extent simulated by each model. On the other hand, decadal prediction experiments, driven by external forcing and initialized with some observed fields, allow us to assess the impact of the representation of the observed initial state on the quality of model predictions. Our analyses show that CMIP5 models respond to the forcing, including the one induced by stratospheric ozone depletion, by reducing the sea ice cover in the Southern Ocean. Some simulations display an increase in sea ice extent. However, models strongly overestimate the variability of sea ice extent and the initialization methods currently used in models do not improve systematically the simulated trends in sea ice extent. On the basis of those results, a critical role of the internal variability in the observed increase in the sea ice extent in the Southern Ocean could not be ruled out but current models results appear inadequate to test more precisely this hypothesis.

1 Introduction

The way climate models reproduce the observed characteristics of sea ice has received a lot of attention (e.g. Flato, 2004; Arzel et al., 2006; Parkinson et al., 2006; Lefebvre

TCD
6, 3539–3573, 2012
CMIP5 1979–2005 Southern Ocean sea ice
V. Zunz et al.

and Goosse, 2008a; Sen Gupta et al., 2009). One conclusion of those studies is that the models skill is higher in the Northern Hemisphere than in the Southern Hemisphere. In particular, simulations performed for the 3rd Coupled Model Intercomparison Project (CMIP3) are generally able to reproduce relatively well the timing of the seasonal cycle of Southern Ocean sea ice extent but fail in simulating the observed amplitude (Parkinson et al., 2006). Furthermore, the models are usually unable to simulate the observed increase in Southern Ocean sea ice extent (e.g. Arzel et al., 2006; Parkinson et al., 2006), which is estimated to be of $11\,200 \pm 2680\,\mathrm{km}^2\,\mathrm{yr}^{-1}$ between 1979 and 2006 (Comiso and Nishio, 2008). At a regional scale, the 1979–2006 trend in observed sea ice extent is positive in all the sectors of the Southern Ocean, except in the Bellingshausen-Amundsen Seas sector, and the Ross Sea sector exhibits the largest positive trend (e.g. Cavalieri and Parkinson, 2008; Comiso and Nishio, 2008). Lefebvre and Goosse (2008a) have studied the trend simulated by several CMIP3 models in the different sectors of the Southern Ocean and they have shown that these models were not able to reproduce this observed spatial structure.

The potential causes of the observed increase in sea ice extent are still debated. Several studies pointed out a relationship between stratospheric ozone depletion over the past few decades (Solomon, 1999) and changes in the atmospheric circulation at high latitudes (e.g. Turner et al., 2009; Thompson et al., 2011). Variations of sea ice extent in the Southern Ocean are in turn influenced by changes in the atmosphere circulation (e.g. Holland and Raphael, 2006; Goosse et al., 2009b). However, the link between atmospheric circulation and the sea ice extent integrated over the Southern Ocean is not straightforward (e.g. Lefebvre and Goosse, 2008b; Stammerjohn et al., 2008; Landrum et al., 2012) and, in their modelling study, Sigmond and Fyfe (2010) came to the conclusion that the stratospheric ozone depletion does not lead to an increase in the sea ice extent. A second potential cause of the observed expansion of sea ice cover relies on an enhanced stratification of the ocean which would inhibit the heat transfer to the surface. This strengthened stratification is mainly due to a freshening of the surface water, itself triggered by an increase in the precipitation over the

Southern Ocean, the melting of the ice shelf and changes in the production and transport of sea ice (e.g. Bitz et al., 2006; Zhang, 2007; Goosse et al., 2009b; Kirkman and Bitz, 2010). Liu and Curry (2010) pointed out that an enhanced hydrological cycle may also increase the snowfalls at high latitudes in the Southern Ocean. In that case, the snow cover on thicker sea ice would raise the surface albedo, strengthen the insulation between the atmosphere and the ocean, and thus would protect the sea ice from melting. Another hypothesis suggests that the positive trend in the Southern Ocean sea ice extent could arise from the low frequency internal variability of the system that could mask the general warming signal in the Southern Ocean. Indeed, the period spanning the last 40 yr during which sea ice cover slightly expanded in the Southern Ocean might follow a large melting that may have happened before 1979 (e.g. de la Mare, 1997, 2009; Cavalieri et al., 2003; Curran et al., 2003; Cotté and Guinet, 2007; Goosse et al., 2009b). However, the lack of observations makes it difficult to confirm this hypothesis.

As a consequence, the general failure of models to simulate properly the observed trend may be due to a misrepresentation of the response of the circulation and/or of the hydrological cycle to the forcing. However, the potential influence of the internal variability and of its representation in models must be assessed too. In this framework, the goal of this paper is to test two related hypotheses. First, models may not reproduce adequately the variability of the sea ice extent in the Southern Ocean and may thus not be able to take into account its potential contribution to the trend. Second, several models may be out of phase with the real system and simulate a decrease in sea ice extent where the real sea ice cover is actually expanding.

To test these two hypotheses, we examine outputs from general circulation models (GCMs) following the 5th Coupled Model Intercomparison Project (CMIP5) protocol. We deal with two kinds of simulations: historical and hindcast (or decadal) simulations. The first ones are driven by external forcing and are initialized without observational constraints. They are used to assess how well each model simulates the observed mean state, variability and trends in sea ice concentration and extent. The objective is

TCD
6, 3539–3573, 2012

to study the possible links between the internal variability of the system and the simulated trend in sea ice extent. Analyzing the mean state also appears to be important here because of its impact on the simulated variability (e.g. Goosse et al., 2009a). In addition to those points related to the variability of the system, the way stratospheric ozone is taken into account in models is also discussed to estimate if this has a significant impact on the simulated trends.

The second kind of simulations, the hindcasts, are also driven by external forcing but, in contrast to the historical simulations, are initialized through data assimilation of observations. Consequently, these simulations allow us to assess how the state of the system in the early 80's impacts on the variability of the models and on their representation of the trend over the last 30 yr. Idealized model studies have shown high potential predictability at decadal time scale in the Southern Ocean (e.g. Latif et al., 2010), i.e. models have deterministic decadal variability, in particular for surface temperatures (Pohlmann et al., 2004). The predictive skill of the models at decadal time scales is also discussed here to see if this potential predictability is confirmed in real applications.

A rapid investigation of the results of CMIP5 models has shown that, in agreement with previous studies related to CMIP3 models (e.g. Lefebvre and Goosse, 2008a), current GCMs fail in simulating the spatial structure of the observed trend in sea ice extent. This leads us to focus on the sea ice extent in the whole Southern Ocean rather than in the individual sectors. Models and observation data are briefly presented in Sect. 2. The time period we analyze is limited by the available observations. For the Southern Ocean, validation data are quite sparse before 1979. We therefore examine outputs between 1979 and 2005. Results provided by models historical simulations are presented and discussed in Sect. 3. The analyses of hindcast simulations are described in Sect. 4. Finally, Sect. 5 summarizes our results and proposes conclusions.

2 Models and observation data

Models data were obtained from the CMIP5 (Taylor et al., 2011) multi-model ensemble: http://pcmdi3.llnl.gov/esgcet/home.htm. We have analysed results of historical simulations from 24 models which have the required data available. Among these models, 10 of them provide results for hindcast simulations. Both historical and hindcast simulations consist in ensemble simulations of various sizes. Models and their respective modeling groups are listed in Table 1, along with the number of members in each model historical and hindcast simulations. The models have different spatial resolution and representation of physical processes. The spatial resolution of models components is summarized in Table S1 of the Online Supplement Table of this paper. A reference is also given for more complete documentation.

We give specific information on the treatment of ozone in Table 2, as a basis for the discussion presented in Sect. 3.3. CNRM-CM5, GFDL-CM3, MIROC-ESM-CHEM and MRI-CGCM3 have an interactive chemistry in their atmospheric component that is activated in CMIP5 simulations. The interactive chemistry of CCSM4, IPSL-CM5A-LR and IPSL-CM5A-MR is deactivated in their CMIP5 simulations but it is used in an offline simulation that allows to compute the ozone dataset then prescribed in the CMIP5 simulations. The AC&C/SPARC ozone database (Cionni et al., 2011) is used to prescribe ozone in most of the models without an interactive chemistry. In this database, stratospheric ozone for the period 1979–2009 is zonally and monthly averaged. It depends on the altitude and it takes solar variability into account. Whether they have interactive chemistry or prescribed stratospheric ozone, the 24 models analyzed in this study thus take into account the stratospheric ozone depletion in their historical simulations. This is an improvement since the CMIP3 simulations. Indeed, nearly half of the CMIP3 models prescribed a constant ozone climatology (Son et al., 2008). Nevertheless, some of the models have a coarse atmosphere resolution which sometimes does not encompass the whole stratosphere. In that case, processes related to the interaction between radiation and ozone as well as the exchange between the stratosphere and the troposphere may be represented rather crudely.

The hindcast simulations were initialized from a state that has been obtained through a data assimilation procedure, i.e. constrained to be close to some observed fields. There is a large panel of data assimilation methods but most of the models involved in CMIP5 assimilate observations through a nudging. This method consists in adding to the model equations a term that slightly pulls the solution towards the observations (Kalnay, 2007). MIROC4h and MIROC5 incorporate observations in their data assimilation experiments by an incremental analysis update (IAU). Details about this method can be found in Bloom et al. (1996). Table 3 summarizes the data assimilation method corresponding to each model, as well as the variable it assimilates. The relevant documentation were not available to us for CCSM4, FGOALS-g2 and MRI-CGCM3. All the models for which we have the adequate information, except BCC-CSM1.1 and CNRM-CM5, assimilate anomalies. Those anomalies are calculated for both model and observations by subtracting their respective climatology, computed over the same reference period. Working with anomalies does not prevent model biases but it avoids the initialization of the model with a state which is too far from its own climatology and thus limits model drift (e.g. Pierce et al., 2004; Smith et al., 2007; Troccoli and Palmer, 2007; Keenlyside et al., 2008; Pohlmann et al., 2009), as discussed in Sect. 4.

A model skill is measured through their representation of the sea ice concentration (the fraction of grid cell covered by sea ice) and sea ice extent (the sum of the areas of all grid cells having an ice concentration of at least 15 %). We consider the sea ice extent over the whole Southern Ocean and for models, it has been calculated on the original models grids. For each model providing an ensemble of simulations, the model mean is the average over the members belonging to the ensemble. The multi-model mean is then derived by computing the mean of the individual models means, without applying any weighting to the models. Sea ice concentration comes from the satellite observation of the National Snow and Ice Data Centre (NSIDC) (Comiso, 1999, updated 2008). The sea ice extent is then derived from this data set following the method described in Cavalieri et al. (1999) and applied by Cavalieri and Parkinson (2008) for the period 1979–2006.

3 Historical simulations

3.1 Mean state and variability

In a first step, we analyze the mean sea ice concentration over the period 1979–2005. To do so, Fig. 1 shows the multi-model mean of sea ice concentration in the Southern Ocean and compares the simulated sea ice edge to the observed one. Results are given for February, the month during which the observed sea ice cover reaches its minimum, and September which corresponds to the maximum of observed sea ice extent. In February, the multi-model mean underestimates the sea ice cover in the Belligshausen and Amundsen Seas as well as in the eastern part of the Ross Sea. In the Western Ross Sea and in small parts of the Weddell Sea and of the Indian Ocean sector, the multi-model mean overestimates the sea ice extent. In September, the shape of the sea ice edge computed from multi-model mean roughly fits the observations. However, the multi-model mean overestimates the sea ice cover everywhere except in the Indian Ocean sector and in the Eastern part of the Ross Sea sector.

This reasonable multi-model mean extent is the result of the average of a wide range of individual behaviors. To account for this variety of mean model states, we plotted, for individual models, the mean of sea ice extent of each month of the year during the period 1979–2005. Figure 2a confirms that the multi-model mean fits quite well the observations, especially during winter months. However, the seasonal cycle of sea ice extent of the various models is largely spread around the observations and the timing of the minimum/maximum sea ice extent varies from one model to the other. In summer, 16 of the models underestimate the sea ice extent. In particular, CNRM-CM5 and MIROC5 are nearly sea ice free during summer. The latter strongly underestimates the ice extent all over the year and its winter sea ice extent is smaller than some models summer sea ice extent. On the contrary, CCSM4 and CSIRO-Mk3.6.0 overestimate the sea ice extent during the whole year, especially during summer. In winter, when the simulated sea ice cover reaches its maximum, the sea ice extent ranges from approximately 5 to 24 millions km^2 while the observations display a sea ice extent of about 17 millions km^2.

Since the internal variability of the climate system may also have played a role in the observed expansion of sea ice cover, we assess its representation in models by computing the standard deviation of the sea ice extent for each month of the year, over the period 1979–2005 (Fig. 2b). Here, to obtain both the ensemble mean of each model and the multi-model mean of standard deviations, an average of the individual standard deviations has been performed. We have chosen to detrend data before computing the standard deviation in order to suppress the direct impact of a trend on the standard deviation that could obscure our analysis of the potential links between those two variables discussed in Sect. 3.2. The monthly standard deviation indicates that the variability strongly differs between models. In February, 15 models have a standard deviation higher than the observed one and all of the 24 models overestimate the standard deviation during September. Consequently, the multi-model mean of standard deviations does not fit very well the observations. It overestimates the standard deviation all over the year, particularly during winter. The interannual variability in some models is significantly larger during winter months than during summer months. As a result, these models have a pronounced seasonal cycle of their standard deviation, in contrast to the observations, which display a relatively constant value throughout the year.

The analysis of Fig. 2b tells us two important things. On the one hand, it points out the inability of the majority of models to reproduce the observed interannual variability. In particular, they all overestimate the winter interannual variability. On the other hand, it highlights the fact that some models are characterized by a very different magnitude of the interannual variability from one season to the other. In order to avoid a loss of

TCD
6, 3539–3573, 2012

information, we have thus chosen in the following analysis to work with seasonal mean rather than with annual mean and to treat the summer and winter separately.

3.2 Trend over the period 1979–2005

For the historical simulations, we have computed for each member of the ensemble the trend from 1979 to 2005 of summer (average of January, February and March) and winter (average of July, August and September) sea ice extent. In addition to a direct evaluation of model skill, one of our goals is to analyse if a relationship can be established between the ability to reproduce the observed trend and the mean state and interannual variability simulated by the model.

Observations show that the summer sea ice cover expanded between 1979 and 2005, at a rate of approximately 150 000 km^2 per decade. In Fig. 3a, it appears that almost all of the simulations performed with the 24 models fail in simulating the sign of this observed trend. Only two models (GFDL-CM3 and GISS-E2-R) have an ensemble mean with a positive trend while most of them simulate a relatively large negative trend. For four additional models (CCSM4, CSIRO-Mk3.6.0, HadCM3 and MRI-CGCM3), some ensemble members display a positive trend. This points out the importance of considering the spread of the ensemble in order to take into account the variety of possible realizations of one single model before drawing conclusions. The variance could also be quite different between members (Fig. 3b). Besides, the individual means of ensemble members performed with the same model are less scattered (Fig. 3a).

The comparison between the trend, the mean extent and standard deviation does not display any clear link in summer between those variables, some of the models that simulate an increase in the ice extent in at least one of their members overestimating the observed mean and variability, some underestimating it. Figure 3b also underlines the fact that models with little ice during summer often have a small interannual variability of summer sea ice extent, in agreement with results of Goosse et al. (2009a).

TCD
6, 3539–3573, 2012

Moreover, the spread of the sea ice extent trends and standard deviations of members belonging to one model ensemble grows with the mean summer sea ice extent.

Winter sea ice extent has also increased between 1979 and 2005, by approximately 85 000 km^2 per decade. Two models have an ensemble mean whose trend is positive: GFDL-CM3 and IPSL-CM5A-MR (Fig. 3c). The ensemble mean of GFDL-CM3 (5 members) has a positive trend which is close to the observed one but it strongly underestimates the mean winter sea ice extent. It is also an ensemble whose members are highly scattered along the trend axis, three having a positive trend (from approximately 500×10^3 to $1300 \times 10^3\,km^2\,decade^{-1}$) and two having a negative one (from approximately -250×10^3 to $-1100 \times 10^3\,km^2\,decade^{-1}$). The IPSL-CM5A-MR ensemble is made up of one member only. Its trend and its mean are both close to the observation.

The 22 remaining models all have an ensemble mean showing a decrease of winter sea ice extent. However, as noticed for summer, a few of them have ensemble members displaying positive trends. Two of three BCC-CSM1.1 historical simulation members are close to each other and present a positive trend. The last one has a very negative trend, reaching $-2500 \times 10^3\,km^2\,decade^{-1}$. Contrarily, the mean sea ice extent does not vary much between members, all of of them being larger than the observations. CSIRO-Mk3.6.0 ensemble simulation contains 10 members. They all simulate a mean sea ice extent in winter relatively close to the observations. Only one member shows an increase in Antarctic sea ice extent.

Figure 3d confirms that all the 24 models overestimate the interannual variability in winter. It also underlines the fact that simulations that have a trend close to the observed one have generally a standard deviation which is much larger than the one of the observations. IPSL-CM5A-MR single member, which has a trend and a mean state relatively close to the observations, has a standard deviation greater than 0.8 millions km^2 while the observed standard deviation stands around 0.25 millions km^2. GFDL-CM3 is the model that has the highest standard deviation (around 6 times the standard deviation of the observations). BCC-CSM1.1 also strongly overestimates the standard deviation of winter sea ice extent. Among the models that display a positive trend in winter, CSIRO-Mk3.6.0 is the one with the lower standard deviation.

3.3 Stratospheric ozone

CMIP5 models all include the stratospheric ozone depletion that occurred during the last 30 yr (see Table 2 for details). However, this improvement brought to the stratospheric ozone does not lead to a better representation of the observed increase in Southern Ocean sea ice extent for the ensemble analyzed as a whole, as discussed above.

To go a step further, we discuss if the way stratospheric ozone is treated has an influence on the results. The models with interactive chemistry (activated during the simulation or used in an offline simulation to compute the ozone dataset) and the ones whith higher atmospheric vertical resolution (≥ 35 layers) have on average a slightly smaller extent of sea ice in summer (Fig. 3a, respectively circle and triangle orange symbols). In winter, the models with fine atmospheric resolution underestimate the sea ice extent while the ones with interactive chemistry overestimate it (Fig. 3c). The influence on the trend is hardly detected. This shows that, on average, the inclusion of an interactive chemistry or an increased vertical resolution do not make major differences compared to other models.

Looking now at individual models, we have seen in Sect. 3.2 that CSIRO-Mk3.6.0, GFDL-CM3 and IPSL-CM5A-MR provide results for sea ice extent trend in winter in relatively good agreement with observations but with too high standard deviation for GFDL-CM3 and IPSL-CM5A-MR. CSIRO-Mk3.6.0 has a quite coarse resolution in its atmosphere component (18 vertical layers) and prescribes the ozone from the AC&C/SPARC database. GFDL-CM3 and IPSL-CM5A-MR have a finer resolution (48 and 39 layers, respectively). They both have interactive chemistry but IPSL-CM5A-MR treats the interaction between ozone and climate through a semi offline approach. For this latter model, ozone fields are computed by the atmospheric chemistry model LMDz-REPROBUS in a decoupled simulation and is then used to prescribe ozone in historical simulation (Szopa et al., 2012). Again, from the available ensemble, the representation of ozone in models does not seem to be the dominant factor influencing the simulation of the trend in sea ice extent.

4 Hindcast simulations

4.1 Impact of the initialization on the simulated trends

The models used for the hindcast analysis have been chosen on the basis of the availability of their results. Fortunately, we see on Fig. 2 that these 10 models (dashed lines) constitute a subset which represents reasonably well the variety of general circulation models. In order to outline the effect of the initialization on the simulated trend in sea ice extent, for each model, we have computed the ensemble mean of the trends in hindcast simulations spanning the period 1981–2005, for winter and summer extent, and compared them to the one from historical simulations (i.e. uninitialized), over the same time period. This period has been chosen as no hindcast was started in 1979. Here, the hindcasts were initialized in January 1981 for all the models except HadCM3, whose hindcast was started in November 1980. On Fig. 4 showing the trend in sea ice extent computed from hindcast simulations against the one computed from historical simulations, a dot located on the line $y(x) = x$ means that the trend in hindcast simulation equals the one of historical simulation. If the trend simulated by hindcast is greater (smaller) than the one computed from historical simulation, then the dot will be above (below) the line $y(x) = x$.

Regarding summer sea ice extent (Fig. 4a), the initialization through a data assimilation procedure does not improve systematically the simulated trend. HadCM3, MIROC4h and MRI-CGCM3 hindcasts trends are closer to the observation than are their historical trends but they remain negative. BCC-CSM1.1, CNRM-CM5, IPSL-CM5A-LR and MPI-ESM-LR simulate a more negative trend in their hindcasts than in their historical runs. FGOALS-g2 has a largely positive trend in its hindcast while the

Discussion Paper | Discussion Paper | Discussion Paper | Discussion Paper |

TCD

6, 3539–3573, 2012

CMIP5 1979–2005 Southern Ocean sea ice

V. Zunz et al.

trend in its historical simulation is slightly negative. CCSM4 hindcast displays a slightly positive trend while the one of its historical simulation is negative.

We do not have information about the method used to initialize FGOALS-g2 hindcasts but it forces the simulation to start with a sea ice extent that is much smaller than the model climatology. FGOALS-g2 is among the models that overestimate the sea ice extent all over the year (Fig. 2a) and in its historical simulation, the summer sea ice extent approximately equals 7 millions km^2 while the observed one is of about 4 millions km^2. The initialization method thus likely pushes the solution of the model towards a state with a smaller sea ice cover, to be closer to the observations. Actually, the initialization has such a strong impact on the sea ice extent that the simulations start with a state characterized by a summer sea ice extent of about 2 millions km^2 (not shown), which is even less ice than in the observations. Since the model is not constrained by observations after the initialization anymore, it tends to go back to its climatology, i.e. a state with a larger sea ice extent. This behavior is responsible for the high positive trend computed from hindcast simulations.

A model drift is also obtained in CCSM4 hindcast simulation, which starts with a summer sea ice extent of about 4 millions km^2 (not shown), thus really close to the observed one but far from this model's climatology, standing around 12 millions km^2. Hindcast simulation then goes back towards the model's climatology. In addition, CCSM4 hindcast summer sea ice extent has a much larger standard deviation than has the one of the historical simulation. This could be due to the initial shock that may induce an enhanced interannual variability during the time period required for the model to get stabilized after the initialization.

The larger negative trend simulated by CNRM-CM5 hindcast has a similar origin as the one previously invoked for FGOALS-g2 and CCSM4. Nevertheless, unlike these models, the climatology of CNRM-CM5 is below the one of observations, all over the year (Fig. 2a). CNRM-CM5 assimilates observations by nudging its solution towards raw data of surface and 3-D ocean temperature and salinity. This induces a state with summer sea ice extent larger than in the historical ($\sim$ 1.2 millions km^2 in hindcast – not

TCD
6, 3539–3573, 2012
CMIP5 1979–2005 Southern Ocean sea ice
V. Zunz et al.

shown – and ~0.1 millions km^2 in historical for summer sea ice extent). After this initial shock, the solution goes back towards the model's climatology, introducing a strongly decreasing artificial trend.

Like CNRM-CM5, BCC-CSM1.1 is initialized through a nudging of raw data, of 3-D ocean temperature only. BCC-CSM1.1 model's climatological sea ice extent is larger than the one of the observation (except in February). However, after the initialization, BCC-CSM1.1 hindcast displays growth of its summer sea ice extent during the first 5 yr of the simulation (from approximately 4 to 7 millions km^2) followed by a decrease of the summer sea ice extent until the end of the simulation, down to a value of about 4 millions km^2 (not shown). The assimilation procedure may therefore be partly responsible of the drift of the initialized simulation.

Similarly, for winter sea ice extent, the initialization with observations does not systematically lead to a simulated trend in better agreement with observations. Figure 4b shows that hindcast simulations of MIROC4h, MIROC5 and MRI-CGCM3 have trends that are slightly closer to the observation than are the historical trends. The 7 other models perform worse or do not offer any improvement when they are initialized with observations. As in the case of summer sea ice extent (Fig. 4a), FGOALS-g2 simulates a large positive trend in its winter sea ice extent when it is initialized with observations and CNRM-CM5 has a more negative trend in its hindcast, for the same reasons as the one proposed above. For BCC-CSM1.1, the hindcast trend in winter sea ice extent do not experience large change compare to historical trend.

Results presented in Fig. 4 show that the initialization of models through data assimilation of observation does not bring significant improvement on the simulated trend. When raw data are used instead of anomalies, the initialization apparently deteriorates the trend in sea ice extent simulated by models, as it has been discussed for BCC-CSM1.1, CNRM-CM5 and FGOALS-g2. Corrections can be introduced to take into account that kind of biases (e.g. Troccoli and Palmer, 2007; Vannitsem and Nicolis, 2008). Nevertheless, such a procedure requires a larger amount of initialized simulations

TCD
6, 3539–3573, 2012

spanning several decades and proposing one for sea ice and analyzing how it would impact on the analysis of the trend is out of the scope of our study.

4.2 Correlation between models and observations

The forecast skill of the models can also be assessed by analyzing the prediction a few years ahead. To do so, for each model, we computed the anomaly correlation coefficient used in Pohlmann et al. (2009):

$$\mathrm{COR}(t) = \frac{\sum_{i=1}^{N}\sum_{j=1}^{M}\left[x_{ij}(t)-\bar{x}\right]\left[o_i(t)-\bar{o}\right]}{\sqrt{\sum_{i=1}^{N}\sum_{j=1}^{M}\left[x_{ij}(t)-\bar{x}\right]^2\sum_{i=1}^{N}M\left[o_i(t)-\bar{o}\right]^2}} \tag{1}$$

where t is the lead time (in years), x_{ij} are the hindcast simulations, i is the ensemble index (different indices correspond to different times when the hindcast simulations are started) and j is the index of the member belonging to the ensemble i. N is the number of ensembles and M is the number of members within each ensemble. o_i is the observation covering the time period spanned by the ensemble i. The overbar stands for the climatological mean of the uninitialized (historical) simulation and of the observations, over the analyzed period (here 1981–2005).

The correlation between hindcast simulations and observations is shown for summer (Fig. 5) and winter (Fig. 6) sea ice extent. This correlation has been computed from a series of 4 hindcasts ensemble simulations, initialized every 5 yr between January 1981 and January 1996 (every 5 yr between November 1980 and November 1995 for HadCM3). The 95 % significance level is computed using a t-test. This significance level varies from one model to another because of the different number of members in each model ensemble (see Table 1).

In summer, none of the 10 models analyzed here has a significant correlation for the first year after initialization (Fig. 5). HadCM3, IPSL-CM5A-LR and MIROC4h never outstrip the 95 % significant level. The 7 remaining models present one or two peaks

TCD
6, 3539–3573, 2012

of significant correlation several years after the initialization and almost all the models have a negative correlation during most of the 10 yr. The emergence of correlation later on in the simulation can occur randomly or it might still be a consequence of the initialization. Indeed, models might undergo an initial shock due to the initialization procedure before getting stabilized and benefit from the initialization. For winter sea ice extent (Fig. 6), the correlation is significantly positive during the first year for CCSM4, MIROC5 and MPI-ESM-LR models, indicating some predictive skill. Then the correlation decreases and reaches negative values. A negative correlation is also found in the other models. The significant correlation after one year in three models in winter likely arises from the initialization but the memory of the system is apparently not sufficient to keep a significant correlation during the following years. Unlike in the Arctic, sea ice around the Antarctic is relatively young. It disappears almost entirely during the melting season and recovers during winter months, preventing this sea ice to retain information from initialization. The ocean can keep the information over longer periods but in the available experiments, its role appears weak during the first year after initialization while it may be responsible for the emergence of correlation several years after initialization, for both summer and winter sea ice extent, through local interactions or teleconnections with remote areas.

In any case, the skill of model predictions for Southern Ocean sea ice extent is quite poor compared to the one obtained for other variables. For instance, Kim et al. (2012) have analyzed hindcasts results from seven CMIP5 models and have shown that these models have a high skill in forecasting surface temperature anomalies over the Indian, North Atlantic and Western Pacific Ocean, up to 6–9 yr ahead. Matei et al. (2012a) have pointed out a significant correlation between hindcast and observations for the Atlantic Meridional Overturning Circulation (AMOC) strength at 26.5° N up to 4 yr ahead.

TCD
6, 3539–3573, 2012

5 Summary and conclusions

We have analyzed results of historical and hindcast simulations from the 24 models available to date, following the CMIP5 protocol. This is still a small ensemble but we can consider that it is diverse enough to constitute a reasonable sample to draw conclusions about current models behavior in the Southern Ocean.

The multi-model mean reproduces well the observed summer and winter sea ice edge as well as the annual cycle of sea ice extent. The skill of individual models is much lower. The majority of the biases in the simulated Southern Ocean sea ice highlighted for CMIP3 models persist for the CMIP5 ones. Furthermore, all the models analyzed here overestimate the variability of the sea ice extent in winter. In addition, we saw that, in contrast to observations, the variability in some models can vary significantly from one season to the other. We thus have chosen to analyze seasonal means rather than annual mean but the conclusions are similar whether we consider summer or winter sea ice extent.

Only very few simulations used in this study are able to reproduce the observed increasing trend in sea ice extent during the last decades. Unfortunately, models with a correct sign of the trend in sea ice extent have either a climatological mean which is far from the observations or a too high interannual variability and ensemble spread, or even both. None of the CMIP5 models provide thus a reasonable estimate of all the main characteristics of the sea ice cover over the last decades in the Southern Ocean, in contrast to the Arctic (e.g. Massonnet et al., 2012). Nevertheless, the analysis of the ensemble has allowed us to reach insightful conclusions.

Firstly, the response of the models to the forcing induces a decrease in ice extent. The only models that display in ensemble mean a positive value have such a large variability that the sign of the trend is not robust. Besides, Landrum et al. (2012) have pointed out that large interannual variability in simulated sea ice concentration leads to late 20th Century trends in sea ice concentration that are not always statistically significant for individual members. Our analysis of stratospheric ozone representation in the different models shows that the inclusion of stratospheric ozone depletion in all the models for which we have the relevant informations (compare to half of the models in CMIP3) does not improve the simulated trend in sea ice extent in the Southern Ocean. Moreover, models with interactive chemistry or with higher atmospheric vertical resolution do not provide better results than the other ones.

Secondly, some ensemble members of a few models display a positive trend in sea ice extent over the last decades. This may indicate that internal variability played a significant role in the observed increase. However, the validity of this hypothesis is still very uncertain because of the systematic biases in the model representation of the mean state and of the variability. For instance, a very large variability increases the probability to have a positive trend by chance among several ensemble members. Even if the model does not reproduce adequately the forced response, this then would overemphasize the role of the interannual variability in observation compared to the one of the forcing. Future ensemble simulations with more members could shed light on this issue.

Thirdly, if the internal variability is important, a correct initialization of the model state may lead to a better agreement with data. In this hypothesis, constraining the model with observations would put the system in a state that favors an increase in ice extent, for instance because of a more stratified or colder ocean. However, results from hindcast simulations have shown that there is no systematic improvement of the simulation of sea ice extent observed trend. Previous studies (e.g. Latif et al., 2010) demonstrated that models have a high potential predictability in the Southern Ocean region at decadal time scale, i.e. there exists in models deterministic decadal variability. The test in real conditions has not shown such predictability for sea ice extent. This may be due to some inadequate representation of physics and/or feedbacks in models but also to the initialization procedure. Indeed, observations required to initialize properly the system are quite sparse in that area and the time period they cover is relatively short. Furthermore, data assimilation methods used in general circulation models are essentially based on a nudging. Our study has shown that these methods are, in some cases, not suitable for the initialization in the Southern Ocean region. Improvement may thus be expected if more sophisticated methods are applied and systematically tested in the Southern Ocean.

Supplementary material related to this article is available online at: http://www.the-cryosphere-discuss.net/6/3539/2012/tcd-6-3539-2012-supplement.pdf.

Acknowledgements. We acknowledge the World Climate Research Programme's Working Group on Coupled Modelling, which is responsible for CMIP, and we thank the climate modeling groups (listed in Table 1 of this paper) for producing and making available their model output. For CMIP the US Department of Energy's Program for Climate Model Diagnosis and Intercomparison provides coordinating support and led development of software infrastructure in partnership with the Global Organization for Earth System Science Portals. We thank J. Jungclaus from the Max Planck Institute for Meteorology (Hamburg, Germany) for his useful advice and his help in the analysis of the MPI model results. We also thank S. Dubinkina for her help with this manuscript. V. Z. is Research Fellow with the Fonds pour la formation à la Recherche dans l'Industrie et dans l'Agronomie (FRIA-Belgium). H. G. and F. M are Senior Research Associate and Research Fellow with the Fonds National de la Recherche Scientifique (F.R.S.-FNRS-Belgium), respectively. This work is supported by the F.R.S.-FNRS and by the Belgian Federal Science Policy Office (Research Program on Science for a Sustainable Development).

TCD
6, 3539–3573, 2012

CMIP5 1979–2005 Southern Ocean sea ice

V. Zunz et al.

References

Arzel, O., Fichefet, T., and Goosse, H.: Sea ice evolution over the 20th and 21st centuries as simulated by current AOGCMs, Ocean Model., 12, 401–415, doi:10.1016/j.ocemod.2005.08.002, 2006. 3540, 3541

Bitz, C. M., Gent, P. R., Woodgate, R. A., Holland, M. M., and Lindsay, R.: The influence of sea ice on ocean heat uptake in response to increasing CO_2, J. Climate, 19, 2437–2450, doi:10.1175/JCLI3756.1, 2006. 3542

Bloom, S. C., Takacs, L. L., da Silva, A. M., and Ledvina, D.: Data assimilation using incremental analysis updates, Mon. Weather Rev., 124, 1256–1271, 1996. 3545

Cavalieri, D. J. and Parkinson, C. L.: Antarctic sea ice variability and trends, 1979–2006, J. Geophys. Res., 113, C07004, doi:10.1029/2007JC004564, 2008. 3541, 3546, 3569, 3570, 3571

Cavalieri, D. J., Parkinson, C. L., Gloersen, P., Comiso, J. C., and Zwally, H. J.: Deriving long-term time series of sea ice cover from satellite passive-microwave multisensor data sets, J. Geophys. Res., 104, 15803–15814, doi:10.1029/1999JC900081, 1999. 3546

Cavalieri, D. J., Parkinson, C. L., and Vinnikov, K. Y.: 30-Year satellite record reveals contrasting Arctic and Antarctic decadal sea ice variability, Geophys. Res. Lett., 30, 1970, doi:10.1029/2003GL018031, 2003. 3542

Chikamoto, Y., Kimoto, M., Ishii, M., Mochizuki, T., Sakamoto, T., Tatebe, H., Komuro, Y., Watanabe, M., Nozawa, T., Shiogama, H., Mori, M., Yasunaka, S., and Imada, Y.: An overview of decadal climate predictability in a multi-model ensemble by climate model MIROC, Clim. Dynam., doi:10.1007/s00382-012-1351-y, in press, 2012. 3567

Cionni, I., Eyring, V., Lamarque, J. F., Randel, W. J., Stevenson, D. S., Wu, F., Bodeker, G. E., Shepherd, T. G., Shindell, D. T., and Waugh, D. W.: Ozone database in support of CMIP5 simulations: results and corresponding radiative forcing, Atmos. Chem. Phys., 11, 11267–11292, doi:10.5194/acp-11-11267-2011, 2011. 3544, 3566

Comiso, J. C.: Bootstrap Sea Ice Concentrations from Nimbus-7 SMMR and DMSP SSM/I, 1979–2007, Digital media, 1999, updated, 2008. 3545, 3568

Comiso, J. C. and Nishio, F.: Trends in the sea ice cover using enhanced and compatible AMSR-E, SSM/I, and SMMR data, J. Geophys. Res., 113, C02S07, doi:10.1029/2007JC004257, 2008. 3541

Cotté, C. and Guinet, C.: Historical whaling records reveal major regional retreat of Antarctic sea ice, Deep-Sea Res. Pt. I, 54, 243–252, 2007. 3542

Curran, M. A. J., van Ommen, T. D., Morgan, V. I., Phillips, K. L., and Palmer, A. S.: Ice core evidence for Antarctic Sea ice decline since the 1950s, Science, 302, 1203–1206, 2003. 3542

de la Mare, W. K.: Abrupt mid-twentieth-century decline in Antarctic sea-ice extent from whaling records, Nature, 389, 57–60, doi:10.1038/37956, 1997. 3542

de la Mare, W. K.: Changes in Antarctic sea-ice extent from direct historical observations and whaling records, Climatic Change, 92, 461–493, doi:10.1007/s10584-008-9473-2, 2009. 3542

Donner, L. J., Wyman, B. L., Hemler, R. S., Horowitz, L. W., Ming, Y., Zhao, M., Golaz, J.-C., Ginoux, P., Lin, S. J., Schwarzkopf, M. D., Austin, J., Alaka, G., Cooke, W. F., Delworth, T. L., Freidenreich, S. M., Gordon, C. T., Griffies, S. M., Held, I. M., Hurlin, W. J., Klein, S. A., Knutson, T. R., Langenhorst, A. R., Lee, H.-C., Lin, Y., Magi, B. I., Malyshev, S. L., Milly, P. C. D., Naik, V., Nath, M. J., Pincus, R., Ploshay, J. J., Ramaswamy, V., Seman, C. J., Shevliakova, E., Sirutis, J. J., Stern, W. F., Stouffer, R. J., Wilson, R. J., Winton, M., Wittenberg, A. T., and Zeng, F.: The dynamical core, physical parameterizations, and basic simulation characteristics of the atmospheric component AM3 of the GFDL Global Coupled Model CM3, J. Climate, 24, 3484–3519, doi:10.1175/2011JCLI3955.1, 2011. 3566

Flato, G. M.: Sea-ice and its response to CO_2 forcing as simulated by global climate models, Clim. Dynam., 23, 229–241, doi:10.1007/s00382-004-0436-7, 2004. 3540

Gao, F., Xin, X., and Wu, T.: Study on the prediction of regional and global temperature in decadal time scale with BCC_CSM1.1, Chin. J. Atmos. Sci., in press, 2012. 3567

Goosse, H., Arzel, O., Bitz, C. M., de Montety, A., and Vancoppenolle, M.: Increased variability of the Arctic summer ice extent in a warmer climate, Geophys. Res. Lett., 36, L23702, doi:10.1029/2009GL040546, 2009a. 3543, 3548

Goosse, H., Lefebvre, W., de Montety, A., Crespin, E., and Orsi, A.: Consistent past half-century trends in the atmosphere, the sea ice and the ocean at high southern latitudes, Clim. Dynam., 33, 999–1016, doi:10.1007/s00382-008-0500-9, 2009b. 3541, 3542

Holland, M. and Raphael, M.: Twentieth century simulation of the southern hemisphere climate in coupled models, Part II: Sea ice conditions and variability, Clim. Dynam., 26, 229–245, doi:10.1007/s00382-005-0087-3, 2006. 3541

Kalnay, E.: Atmospheric Modeling, Data Assimilation and Predictability, 4th Edn., Cambridge University Press, Cambridge, 2007. 3545

Kawase, H., Nagashima, T., Sudo, K., and Nozawa, T.: Future changes in tropospheric ozone under Representative Concentration Pathways (RCPs), Geophys. Res. Lett., 38, L05801, doi:10.1029/2010GL046402, 2011. 3566

Keenlyside, N., Latif, M., Jungclaus, J. H., Kornbueh, L., and Roeckner, E.: Advancing decadal-scale climate prediction in the North Atlantic sector, Nature, 453, 7191, doi:10.1038/nature06921, 2008. 3545

Kim, H.-M., Webster, P. J., and Curry, J. A.: Evaluation of short-term climate change prediction in multi-model CMIP5 decadal hindcasts, Geophys. Res. Lett., 39, L10701, doi:10.1029/2012GL051644, 2012. 3555

Kirkman, C. H. and Bitz, C. M.: The effect of the sea ice freshwater flux on Southern Ocean temperatures in CCSM3: deep-ocean warming and delayed surface warming, J. Climate, 24, 2224–2237, doi:10.1175/2010JCLI3625.1, 2010. 3542

Landrum, L., Holland, M. M., Schneider, D. P., and Hunke, E.: Antarctic sea ice climatology, variability, and late twentieth-century change in CCSM4, J. Climate, 25, 4817–4838, doi:10.1175/JCLI-D-11-00289.1, 2012. 3541, 3556, 3566

Latif, M., Delworrth, T., Dommenget, D., Drange, H., Hazeleger, W., Hurrell, J., Keenlyside, N., Meehl, G. A., and Sutton, R.: Dynamics of decadal climate variability and implications for its prediction, in: Proceedings of OceanObs'09: Sustained Ocean Observations and Information for Society, 21–25 September 2009, vol. 2, edited by: Hall, J., Harrison, D. E., and Stammer, D., ESA Publication WPP-306, Venice, Italy, 2010. 3543, 3557

Lefebvre, W. and Goosse, H.: Analysis of the projected regional sea-ice changes in the Southern Ocean during the twenty-first century, Clim. Dynam., 30, 59–76, doi:10.1007/s00382-007-0273-6, 2008a. 3540, 3541, 3543

Lefebvre, W. and Goosse, H.: An analysis of the atmospheric processes driving the large-scale winter sea ice variability in the Southern Ocean, J. Geophys. Res., 113, C02004, doi:10.1029/2006JC004032, 2008b. 3541

Liu, J. and Curry, J. A.: Accelerated warming of the Southern Ocean and its impacts on the hydrological cycle and sea ice, P. Natl. Acad. Sci. USA, 107, 14987–14992, 2010. 3542

Massonnet, F., Fichefet, T., Goosse, H., Bitz, C. M., Philippon-Berthier, G., Holland, M. M., and Barriat, P.-Y.: Constraining projections of summer Arctic sea ice, The Cryosphere Discuss., 6, 2931–2959, doi:10.5194/tcd-6-2931-2012, 2012. 3556

Matei, D., Baehr, J., Jungclaus, J. H., Haak, H., Müller, W. A., and Marotzke, J.: Multiyear prediction of monthly mean Atlantic meridional overturning circulation at 26.5° N, Science, 335, 76–79, doi:10.1126/science.1210299, 2012a. 3555

Matei, D., Pohlmann, H., Jungclaus, J. H., Müller, W. A., Haak, H., and Marotzke, J.: Two tales of initializing decadal climate predictions experiments with the ECHAM5/MPI-OM model, J. Climate, doi:10.1175/JCLI-D-11-00633.1, 2012b. 3567

Parkinson, C. L., Vinnikov, K. Y., and Cavalieri, D. J.: Evaluation of the simulation of the annual cycle of Arctic and Antarctic sea ice coverages by 11 major global climate models, J. Geophys. Res., 111, C07012, doi:10.1029/2005JC003408, 2006. 3540, 3541

Pierce, D. W., Barnett, T. P., Tokmakian, R., Semtner, A., Maltrud, M., Lysne, J., and Craig, A.: The ACPI project, element 1: Initializing a coupled climate model from observed conditions, Climatic Change, 62, 13–28, doi:10.1023/B:CLIM.0000013676.42672.23, 2004. 3545

Pohlmann, H., Botzet, M., Latif, M., Roesch, A., Wild, M., and Tschuck, P.: Estimating the decadal predictability of a coupled AOGCM, J. Climate, 17, 4463–4472, doi:10.1175/3209.1, 2004. 3543

Pohlmann, H., Jungclaus, J. H., Köhl, A., Stammer, D., and Marotzke, J.: Initializing decadal climate predictions with the GECCO oceanic synthesis: effects on the North Atlantic, J. Climate, 22, 3926–3938, doi:10.1175/2009JCLI2535.1, 2009. 3545, 3554

Randel, W. J. and Wu, F.: A stratospheric ozone trends data set for global modeling studies, Geophys. Res. Lett., 26, 3089–3092, doi:10.1029/1999GL900615, 1999. 3566

Sen Gupta, A., Santoso, A., Taschetto, A. S., Ummenhofer, C. C., Trevena, J., and England, M. H.: Projected changes to the Southern Hemisphere Ocean and sea ice in the IPCC AR4 climate models, J. Climate, 22, 3047–3078, doi:10.1175/2008JCLI2827.1, 2009. 3541

Sigmond, M. and Fyfe, J. C.: Has the ozone hole contributed to increased Antarctic sea ice extent?, Geophys. Res. Lett., 37, L18502, doi:10.1029/2010GL044301, 2010. 3541

Smith, D. M., Cusack, S., Colman, A. W., Folland, C. K., Harris, G. R., and Murphy, J. M.: Improved surface temperature prediction for the coming decade from a Global Climate Model, Science, 317, 796–799, doi:10.1126/science.1139540, 2007. 3545

Solomon, S.: Stratospheric ozone depletion: a review of concepts and history, Rev. Geophys., 37, 275–316, doi:10.1029/1999RG900008, 1999. 3541

Son, S. W., Polvani, L. M., Waugh, D. W., Akiyoshi, H., Garcia, R., Kinnison, D., Pawson, S., Rozanov, E., Shepherd, T. G., and Shibata, K.: The impact of stratospheric ozone recovery on the Southern Hemisphere Westerly Jet, Science, 320, 1486–1489, 2008. 3544

Stammerjohn, S. E., Martinson, D. G., Smith, R. C., Yuan, X., and Rind, D.: Trends in Antarctic annual sea ice retreat and advance and their relation to El Niño Southern Oscillation and Southern Annular Mode variability, J. Geophys. Res., 113, C03S90, doi:10.1029/2007JC004269, 2008. 3541

Swingedouw, D., Mignot, J., Labtoulle, S., Guilyardi, E., and Madec, G.: Initialisation and predictability of the AMOC over the last 50 years in a climate model, Clim. Dynam., accepted, 2012. 3567

Szopa, S., Balkanski, Y., Schulz, M., Bekki, S., Cugnet, D., Fortems-Cheiney, A., Turquety, S., Cozic, A., Deandreis, C., Hauglustaine, D., Idelkadi, A., Lathiere, J., Lefevre, F., Marchand, M., Vuolo, R., Yan, N., and Dufresne, J.-L.: Aerosol and Ozone changes as forcing for Climate Evolution between 1850 and 2100, Clim. Dynam., submitted, 2012. 3551, 3566

Taylor, K. E., Stouffer, R. J., and Meehl, G. A.: An overview of CMIP5 and the experiment design, B. Am. Meteorol. Soc., 93, 485–498, doi:10.1175/BAMS-D-11-00094.1, 2011. 3544

Thompson, D. W. J., Solomon, S., Kushner, P. J., England, M. H., Grise, K. M., and Karoly, D. J.: Signatures of the Antarctic ozone hole in Southern Hemisphere surface climate change, Nat. Geosci., 4, 741–749, doi:10.1038/ngeo1296, 2011. 3541

Troccoli, A. and Palmer, T. N.: Ensemble decadal predictions from analysed initial conditions, Philos. T. Roy. Soc. A, 365, 2179–2191, doi:10.1098/rsta.2007.2079, 2007. 3545, 3553

Turner, J., Comiso, J. C., Marshall, G. J., Lachlan-Cope, T. A., Bracegirdle, T., Maksym, T., Meredith, M. P., Wang, Z., and Orr, A.: Non-annular atmospheric circulation change induced by stratospheric ozone depletion and its role in the recent increase of Antarctic sea ice extent, Geophys. Res. Lett., 36, L08502, doi:10.1029/2009GL037524, 2009. 3541

Vannitsem, S. and Nicolis, C.: Dynamical properties of model output statistics forecasts, Mon. Weather Rev., 136, 405–419, doi:10.1175/2007MWR2104.1, 2008. 3553

Voldoire, A., Sanchez-Gomez, E., Salas y Mélia, D., Decharme, B., Cassou, C., Sénési, S., Valcke, S., Beau, I., Alias, A., Chevallier, M., Déqué, M., Deshayes, J., Douville, H., Fernandez, E., Madec, G., Maisonnave, E., Moine, M. P., Planton, S., Saint-Martin, D., Szopa, S., Tyteca, S., Alkama, R., Belamari, S., Braun, A., Coquart, L., and Chauvin, F.: The CNRM-CM5.1 global climate model: description and basic evaluation, Clim. Dynam., doi:10.1007/s00382-011-1259-y, in press, 2011. 3566

Watanabe, S., Hajima, T., Sudo, K., Nagashima, T., Takemura, T., Okajima, H., Nozawa, T., Kawase, H., Abe, M., Yokohata, T., Ise, T., Sato, H., Kato, E., Takata, K., Emori, S., and Kawamiya, M.: MIROC-ESM 2010: model description and basic results of CMIP5-20c3m experiments, Geosci. Model Dev., 4, 845–872, doi:10.5194/gmd-4-845-2011, 2011. 3566

Yukimoto, S., Yoshimura, H., Hosaka, M., Sakami, T., Tsujino, H., Hirabara, M., Tanaka, T. Y., Deushi, M., Obata, A., Nakano, H., Adachi, Y., Shindo, E., Yabu, S., Ose, T., and Kitoh, A.: Meteorological Research Institute – Earth System Model Version 1 (MRI-ESM1) – Model Description, Tech. Rep. 64, Meteorological Research Institute, Japan, 2011. 3566

Zhang, J.: Increasing Antarctic sea ice under warming atmospheric and oceanic conditions, J. Climate, 20, 2515–2529, doi:10.1175/JCLI4136.1, 2007. 3542

Table 1. Model name, Institute and number of members in models historical and hindcast simulations.

Model name	Institute ID	Modeling center	Number of members in historical	Number of members in hindcasts
BCC-CSM1.1	BCC	Beijing Climate Center, China Meteorological Administration	3	4
CanESM2	CCCMA	Canadian Centre for Climate Modelling and Analysis	5	–
CCSM4	NCAR	National Center for Atmospheric Research	6	10
CNRM-CM5	CNRM-CERFACS	Centre National de Recherches Meteorologiques / Centre Europeen de Recherche et Formation Avancees en Calcul Scientifique	10	10
CSIRO-Mk3.6.0	CSIRO-QCCCE	Commonwealth Scientific and Industrial Research Organization in collaboration with Queensland Climate Change Centre of Excellence	10	–
EC-EARTH	EC-EARTH	EC-EARTH consortium	1	–
FGOALS-g2	LASG-CESS	LASG, Institute of Atmospheric Physics, Chinese Academy of Sciences and CESS,Tsinghua University	1	3
FGOALS-s2	LASG-IAP	LASG, Institute of Atmospheric Physics, Chinese Academy of Sciences	3	–
GFDL-CM3	NOAA GFDL	NOAA Geophysical Fluid Dynamics Laboratory	5	–
GFDL-ESM2M	NOAA GFDL	NOAA Geophysical Fluid Dynamics Laboratory	1	–
GISS-E2-R	NASA GISS	NASA Goddard Institute for Space Studies	5	–
HadCM3	MOHC	Met Office Hadley Centre	10	10
HadGEM2-CC	MOHC	Met Office Hadley Centre	1	–
HadGEM2-ES	MOHC	Met Office Hadley Centre	1	–
INM-CM4	INM	Institute for Numerical Mathematics	1	–
IPSL-CM5A-LR	IPSL	Institut Pierre-Simon Laplace	4	6
IPSL-CM5A-MR	IPSL	Institut Pierre-Simon Laplace	1	–
MIROC4h	MIROC	Atmosphere and Ocean Research Institute (The University of Tokyo), National Institute for Environmental Studies, and Japan Agency for Marine-Earth Science and Technology	3	3
MIROC5	MIROC	Atmosphere and Ocean Research Institute (The University of Tokyo), National Institute for Environmental Studies, and Japan Agency for Marine-Earth Science and Technology	1	6
MIROC-ESM	MIROC	Japan Agency for Marine-Earth Science and Technology, Atmosphere and Ocean Research Institute (The University of Tokyo), and National Institute for Environmental Studies	3	–
MIROC-ESM-CHEM	MIROC	Japan Agency for Marine-Earth Science and Technology, Atmosphere and Ocean Research Institute (The University of Tokyo), and National Institute for Environmental Studies	1	–
MPI-ESM-LR	MPI-M	Max Planck Institute for Meteorology	3	10 (3 in 30-yr hindcast)
MRI-CGCM3	MRI	Meteorological Research Institute	3	3
NorESM1-M	NCC	Norwegian Climate Centre	3	–

TCD
6, 3539–3573, 2012

Table 2. Summary of atmosphere vertical resolution and stratospheric ozone representation. Models in bold are the ones with an interactive chemistry, activated during the CMIP5 simulations or only activated in an offline simulation used to compute the ozone dataset prescribed in the CMIP5 simulations.

Model name	Atmosphere vertical resolution	Stratospheric ozone
BCC-CSM1.1	26 layers Top layer at 2.9 hPa	Prescribed; AC&C/SPARC ozone database (Cionni et al., 2011).
CanESM2	35 layers Top layer at 1 hPa	Prescribed AC&C/SPARC ozone database (Cionni et al., 2011)
CCSM4	26 layers	Prescribed; Data from an offline simulation of the CAM3.5 model with a fully interactive chemistry (Landrum et al., 2012)
CNRM-CM5	31 layers Top layer at 10 hPa	Interactive chemistry (Voldoire et al., 2011).
CSIRO-Mk3.6.0	18 layers	Prescribed; AC&C/SPARC ozone database (Cionni et al., 2011)
EC-EARTH	62 layers Top layer 5 hPa	Prescribed; AC&C/SPARC ozone database (Cionni et al., 2011)
FGOALS-g2	26 layers	No information available to us.
FGOALS-s2	26 layers Top layer at 2.19 hPa	No information available to us.
GFDL-CM3	48 layers	Interactive chemistry (Donner et al., 2011).
GFDL-ESM2M	24 layers	Prescribed; AC&C/SPARC ozone database (Cionni et al., 2011).
GISS-E2-R	40 layers Top layer at 0.1 hPa	Prescribed; Observational analyses of Randel and Wu (1999).
HadCM3	19 layers	Prescribed; Observational analyses of Randel and Wu (1999)
HadGEM2-CC	60 layers Top layer at 0.006 hPa	Prescribed; AC&C/SPARC ozone database (Cionni et al., 2011).
HadGEM2-ES	38 layers Top layer at 4 hPa	Prescribed; AC&C/SPARC ozone database (Cionni et al., 2011).
INM-CM4	21 layers Top layer at 10 hPa	Prescribed; AC&C/SPARC ozone database (Cionni et al., 2011).
IPSL-CM5A-LR	39 layers Top layer at 0.04 hPa	Prescribed; Data from an offline simulation of the LMDz-REPROBUS model (Szopa et al., 2012).
IPSL-CM5A-MR	39 layers Top layer at 0.04 hPa	Prescribed; Data from an offline simulation of the LMDz-REPROBUS model (Szopa et al., 2012).
MIROC4h	56 layers Top layer at 40 km	Prescribed; Data from an offline simulation of Kawase et al. (2011).
MIROC5	40 layers Top layer at 3 hPa	Prescribed; Data from an offline simulation of Kawase et al. (2011).
MIROC-ESM	80 layers Top layer at 0.003 hPa	Prescribed; Data from an offline simulation of Kawase et al. (2011).
MIROC-ESM-CHEM	80 layers Top layer at 0.003 hPa	Interactive chemistry (Watanabe et al., 2011).
MPI-ESM-LR	47 layers Top layer at 0.01 hPa	Prescribed; AC&C/SPARC ozone database (Cionni et al., 2011).
MRI-CGCM3	48 layers Top layer at 0.01 hPa	Interactive chemistry (Yukimoto et al., 2011).
NorESM1-M	26 layers Top layer at 2.9 hPa	No information available to us.

Table 3. Data assimilation methods used by the 10 models providing hindcast simulations.

Model name	Data assimilation method	References
BCC-CSM1.1	Nudging of 3-D ocean temperature (raw data).	Gao et al. (2012)
CCSM4	Information not available to us	
CNRM-CM5	Nudging of 3-D ocean temperature and salinity (raw data) as a function of depth and space, sea surface temperature and salinity nudging (raw data).	ftp://ftp.cerfacs.fr/pub/globc/exchanges/cassou/Michael/Aspen_CMIP5_wrkshop_cassou_2.ppt
FGOALS-g2	No information available to us.	
HadCM3	Nudging of 3-D ocean temperature and salinity (anomalies), nudging of 3-D atmosphere temperature and wind speed, nudging of surface pressure.	http://www.met.reading.ac.uk/~swr06jir/presentations/JIR_dept_seminar.pptx
IPSL-CM5A-LR	Nudging of sea surface temperature (anomalies).	Swingedouw et al. (2012)
MIROC4h	Incremental analysis update (IAU) of 3-D ocean temperature and salinity (anomalies).	Chikamoto et al. (2012)
MIROC5	Incremental analysis update (IAU) of 3-D ocean temperature and salinity (anomalies).	Chikamoto et al. (2012)
MPI-ESM-LR	Nudging of 3-D ocean temperature and salinity (anomalies), except in the area covered by sea ice.	Matei et al. (2012b)
MRI-CGCM3	No information available to us.	

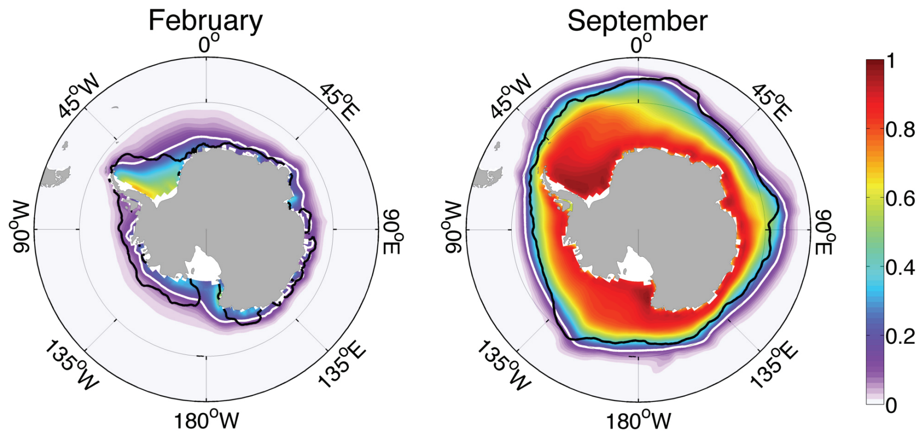

Fig. 1. Multi-model mean of sea ice concentration, computed from historical simulations over the period 1979–2005. White (black) line refers to the sea ice edge, i.e. the 15 % concentration limit of the multi-model ensemble mean (observations, Comiso, 1999, updated 2008).

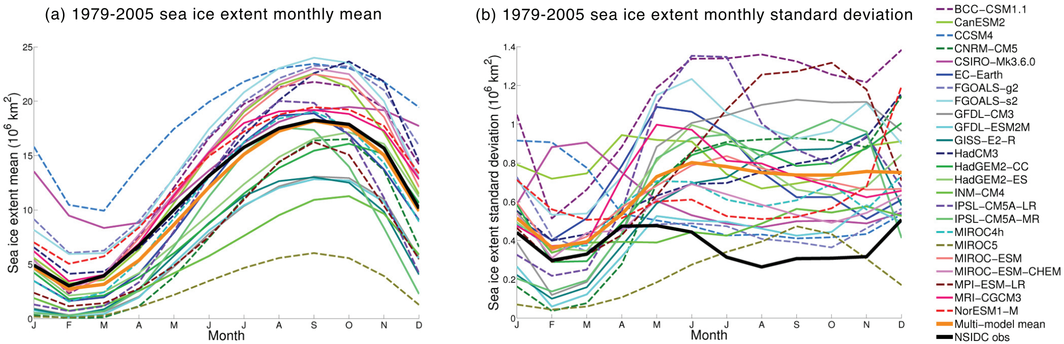

Fig. 2. (a) Monthly mean of Southern Ocean sea ice extent, computed over the period 1979–2005. **(b)** Standard deviation of detrended Southern Hemisphere sea ice extent, computed over the period 1979–2005 for each month of the year. Colors correspond to the ensemble mean of historical simulations from 24 different models. Dashed lines refer to models that provide both historical and hindcast simulations but here, results are only from historical simulations. Orange bold line is the multi-model mean. Black bold line refers to observations (Cavalieri and Parkinson, 2008).

TCD
6, 3539–3573, 2012

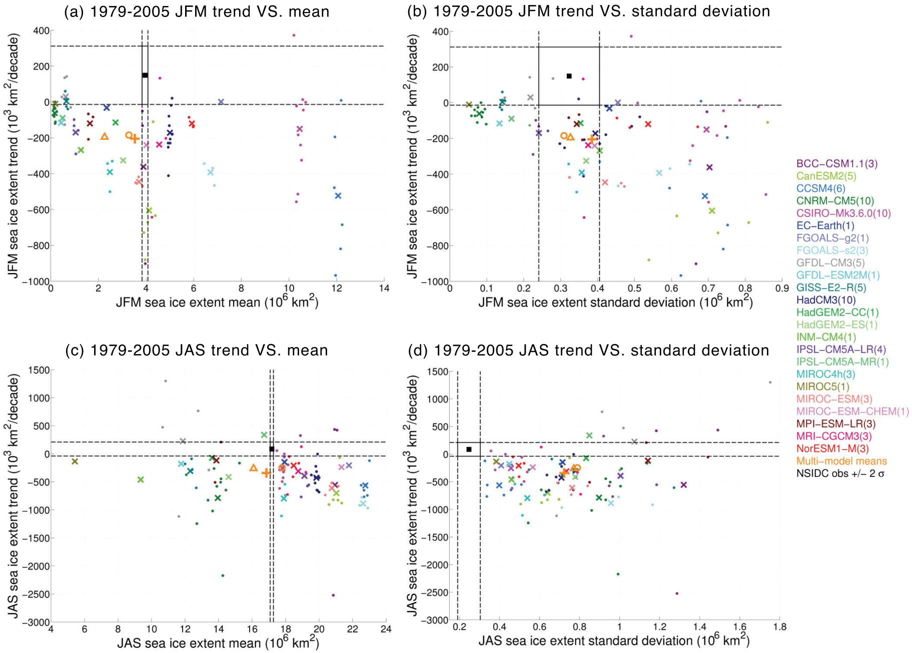

Fig. 3. Sea ice extent trend for the period 1979–2005 over the whole Southern Ocean vs. mean **(a, c)** and standard deviation **(b, d)**. The first row corresponds to summer (JFM), the second to winter (JAS). Colors correspond to historical simulations from 24 different models. Dots refer to model individual members and crosses are for model ensemble mean. The number of members in each model is indicated in brackets. Orange refers to multi-model means: plus sign is for the mean over all of the models, circle sign is for the mean over models with interactive chemistry (in bold in Table 2) and triangle sign is for the mean over models with 35 atmospheric levels or more on the vertical. Black square is for the observations (Cavalieri and Parkinson, 2008).

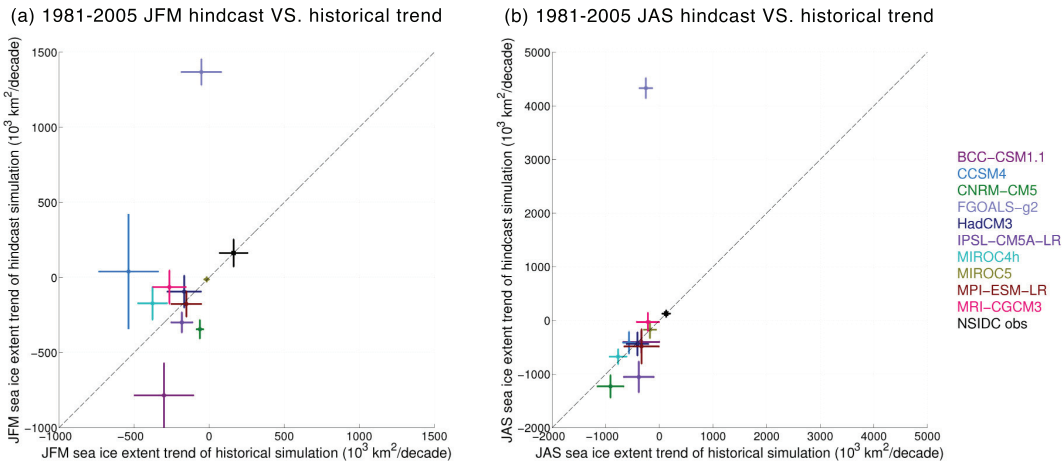

Fig. 4. Hindcast vs. historical Southern Ocean sea ice extent trend for summer **(a)** and winter **(b)**, computed over the period 1981–2005. Colors refer to models ensemble mean. Black square is for the observations (Cavalieri and Parkinson, 2008). Horizontal (vertical) bars show the standard deviation of the trend in the historical (hindcast) simulations. Dashed line represents the line $y(x) = x$.

TCD
6, 3539–3573, 2012

Title Page
Abstract Introduction
Conclusions References
Tables Figures
◀ ▶
Back Close
Full Screen / Esc
Printer-friendly Version
Interactive Discussion

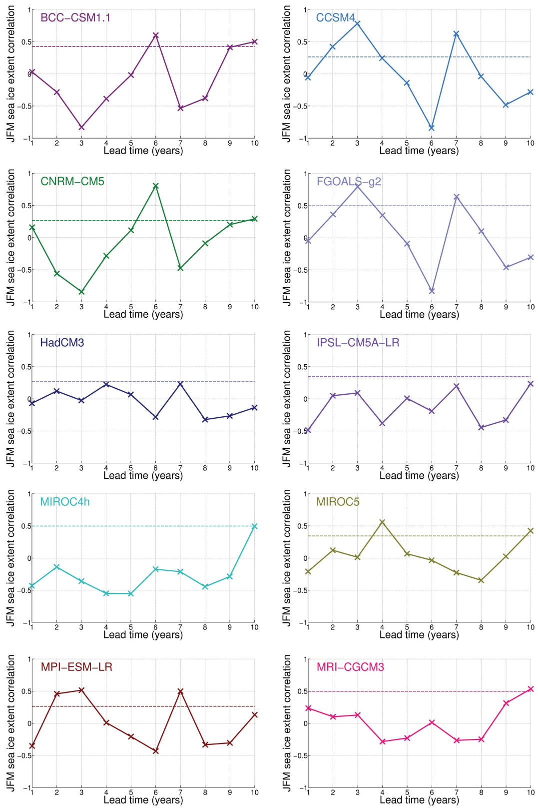

Fig. 5. Correlation between Southern Ocean summer (JFM) sea ice extent in models results and observations. For each model, the correlation is computed from a series of 4 hindcasts ensembles, initialized every 5 yr between January 1981 and January 1996 (between November 1980 and November 1995 for HadCM3). In each plot, the dashed line refers to the 95 % significance level.

TCD
6, 3539–3573, 2012

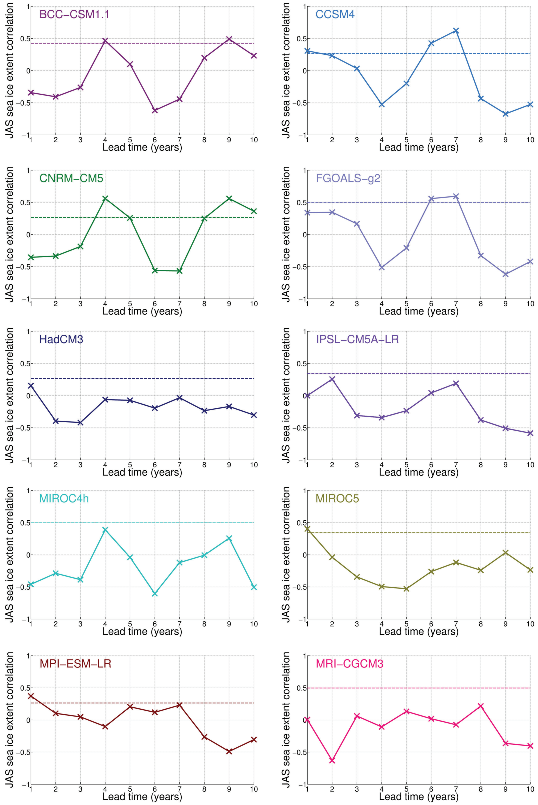

Fig. 6. Correlation between Southern Ocean winter (JAS) sea ice extent in models results and observations. For each model, the correlation is computed from a series of 4 hindcasts ensembles, initialized every 5 yr between January 1981 and January 1996 (between November 1980 and November 1995 for HadCM3). In each plot, the dashed line refers to the 95 % significance level.